FUTURE CLIMATE PROJECTION OF MEGACITIES CONSIDERING URBANIZATION SCENARIOS

Do Ngoc KHANH,[1] Alvin C. G. VARQUEZ[2] and Manabu KANDA[3]

[1]Student Member of JSCE, Dept. of Transdisciplinary Sci. and Eng., Tokyo Institute of Technology
(2-12-1 Ookayama, Meguro-ku, Tokyo, 152-8550, Japan)
E-mail: do.k.aa@m.titech.ac.jp (Corresponding Author)
[2]Member of JSCE, Associate Professor, Dept. of Transdisciplinary Sci. and Eng., Tokyo Institute of Technology
(2-12-1 Ookayama, Meguro-ku, Tokyo, 152-8550, Japan)
E-mail: varquez.a.aa@m.titech.ac.jp
[3]Member of JSCE, Professor, Dept. of Transdisciplinary Sci. and Eng., Tokyo Institute of Technology
(2-12-1 Ookayama, Meguro-ku, Tokyo, 152-8550, Japan)
E-mail: kanda.m.aa@m.titech.ac.jp

Urbanization is an essential, yet underrepresented, parameter when investigating futuristic climate change of cities. The change in 2 m air temperature in August between the 2006–2015 period and the 2046–2055 period for 33 megacities and 10 emerging megacities under RCP8.5 emission forcing and SSP3 was projected with the consideration of both global climate change (using pseudo-global warming method) and local urbanization (using global urban sprawling map, distributed urban morphological parameters, and hourly anthropogenic heat emission dataset).

In newly urbanized area, the urbanization effect will be significant, accounting for (13.5 ± 5.9) % of the total temperature change. In existing urban areas, the effect will vary depending on the current degree of urbanization. When viewed over a regional scale, the effect will be rather insignificant. It was observed in some cities that urbanization effect originating from urban area was advected by the wind to non-urban area located kilometers downwind.

Key Words: climate change, urbanization, global urban climatology

1. INTRODUCTION

It is projected that 60 percent of world population will live in urban areas by 2030 and 8.8 percent will live in urban settlements with the population of at least 10 million which is often referred to as megacities.[1] This is one of the reasons why climatological study at city scale is becoming more important. This kind of study will also help in projecting environmental hazards to human such as heat stress, projecting future energy demand for air conditioning and other projections.

There have been attempts to project future climate for individual cities around the world.[2),3),4),5)] These studies focused on individual cities, some utilized locally available datasets such as land-use dataset[3)] and master plan for future urbanization.[4)] Furthermore, spatial distribution of futuristic projections of urban morphological parameters were not considered in many cases. Studies focused on cities in developing countries are still rare even though urbanization is progressing rapidly in developing countries.

The study of Darmanto et al.,[5)] while focused only on a single city, proposed a framework that relies solely on publicly available global datasets, and therefore can be flexibly extended to any region of interest. In this study, we attempt to scale that approach to project future climate for many cities simultaneously at high resolution using publicly available global datasets. Target cities are 33 existing megacities and 10 cities projected to become megacities by 2030 by the United Nations.[1)] Target for numerical simulation is the mean climate condition in August in the 2006–2015 period and the 2046–2055 period. Our objective is to

- quantify the effect of urbanization on air temperature change at different spatial scale,
- investigate the effect of urbanization in non-urban

areas surrounding urban areas.

2. METHODOLOGY

(1) Meteorological input

The Final Operational Global Analysis dataset published by the National Centers for Environmental Prediction was used as the meteorological input for modeling. Present meteorological input was calculated as the ensemble average of the dataset for all days in August from 2006 to 2015.

Meteorological input for simulation of future scenarios was constructed using the pseudo-global warming (PGW) method.[6] Five General Circulation Model (GCM) members (GFDL-ESM2M, IPSL-CM5A-LR, MIROC-ESM-CHEM, HadGEM2-ES, and NorESM1-M) of CMIP5 were used. The difference between the ensemble average of the GCMs' outputs for the 2046–2055 period and that for the 2006–2015 period was added to the present meteorological input to produce the future meteorological input. Specifically, the difference in wind velocity components, surface temperature, air temperature and geopotential height was added. Emission scenario RCP8.5 was considered. Sea surface temperature was taken from the analysis dataset and the GCMs' outputs.

In each simulation, the meteorological input described above was recycled daily for four consecutive days and inputted to the model to produce a four-day-long output.[7] The first day's output was considered as the model's spinning up period and was discarded. The ensemble of the output of last three days was taken as the simulated climate condition and was used for further analysis.

(2) Urban surface boundary consideration

For the present climate simulation, population density adjusted by nighttime lights[8] were used to modify the MODIS land cover type dataset to put more emphasis on urban land use. Distributed urban morphological parameters were considered in the model following Varquez et al.[9] In addition, hourly-varying anthropogenic heat flux map[10] with point source improvement[11] was used.

For the future climate simulation, population density was projected by combining a logistic model[12] with a global urban sprawling map.[13] Country level GDP and population projection under SSP3 needed as input for the logistic model was obtained from the SSP Public Database.[14),15),16),17] Urban morphological parameters and anthropogenic heat flux map were calculated by the same method with the present case.

(3) Target domains

A modified version of the WRF model v3.3.1 coupled with single-layer urban canopy model was used. This modified version has improvements to consider spatial variations in urban morphological parameters.[9] 41 set of domains were setup for 43 target cities Guangzhou and Shenzhen, Rio de Janeiro and Sao Paulo were grouped into two groups because of they are located close to each other. Each set of domain consists of a coarse domain and a fine domain with the resolutions of 10 km and 2 km respectively. The option of updating sea surface temperature at each input interval was turned off. The domains are listed in Table 1.

(4) Simulated scenarios

We conducted simulation for three scenarios as summarized in Table 2. The present scenario is the basis for model verification and future projection. As for the future scenario, from the construction of input consisting of the global urban sprawling map assuming uncontrolled urban expansion, GDP and population growth projection under SSP3 characterized by high mitigation, adaptation challenges,[14] and highest emission forcing RCP8.5, we assume that the simulated future scenario represents the worst case scenario.

The intermediate scenario considers the change in climate forcing but does not take urbanization (urban sprawling and anthropogenic heat emission change) into consideration. This scenario is used to evaluate the impact of urbanization.

Table 1 List of domains. The number in the brackets following each domain's name is the number of meteorological stations available for model verification for that domain.

Ahmadabad	(2)	Bangalore	(4)	Bangkok	(14)
Beijing	(1)	Bogota	(3)	Buenos Aires	(8)
Cairo	(6)	Chengdu	(2)	Chennai	(3)
Chongqing	(1)	Dar es Salaam	(2)	Delhi	(4)
Dhaka	(7)	Guangzhou	(11)	Ho Chi Minh City	(3)
Hyderabad	(3)	Istanbul	(4)	Jakarta	(7)
Karachi	(2)	Kinshasa	(4)	Kolkata	(14)
Lagos	(7)	Lahore	(3)	Lima	(1)
London	(14)	Los Angeles	(38)	Luanda	(1)
Manila	(15)	Mexico City	(6)	Moscow	(4)
Mumbai	(7)	Nanjing	(2)	New York	(37)
Osaka	(17)	Paris	(11)	Rio de Janeiro	(17)
Seoul	(25)	Shanghai	(5)	Tehran	(4)
Tianjin	(4)	Tokyo	(27)		

Table 2 Simulated scenarios.

Scenario	Urbanization	Climate forcing
Present	present	present
Intermediate	present	future
Future	future	future

3. RESULTS AND DISCUSSIONS

(1) Verification of simulated present climate condition

The simulated present climate condition was compared against the ensemble of observation data. In detail, the simulated 2 m air temperature, which was available hourly, was compared against the ensemble of corresponding observations. Observations from world wide stations were obtained from https://www.ogimet.com and only stations that reported data continuously in the 2006–2015 period were chosen. Refer to Table 1 for the number of stations available for each domain.

Validation result is summarized in Table 3. Overall, the model had a tendency to overestimate 2 m air temperature. However, comparing the bias in daytime and night time, it can be seen that the tendency was significantly stronger in daytime than in night time. At the level of individual cities, RMSEs and biases varied in larger ranges.

We concluded that the performance of the model in reproducing the present climate condition is adequate because of the following reasons:

- The meteorological input was not historical data but the ensemble of historical data,
- Overall and in all breakdowns, Pearson correlation coefficient r indicated that simulated and observed 2 m air temperature were well-correlated,
- 76.1 % of simulated 2 m air temperature lay within one standard deviation of the corresponding observed value and 97.8 % lay within two standard deviations,
- Our approach relied solely on publicly available global input datasets with no adjustments made to adapt to any specific city.

We also concluded that the model is adequate for the following discussion about temperature change between the present and the future because the influence of the bias should be minimized in the difference, and for the discussion about urbanization effect because
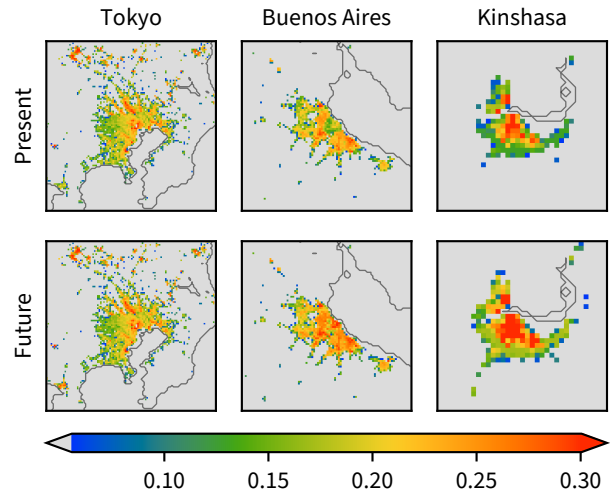

Fig. 1 Plan area index (dimensionless) in the present and future scenario in some domains. Spatial scales are different and omitted.

the effect arises from the difference in urban morphological parameters and urban land use between the intermediate and future scenario both of which have the same climate forcing.

(2) Quantification of urbanization effect

Each domain's spatial mean of change in daily mean 2 m air temperature under different view points (whole domain, old urban, and new urban) is summarized in Table 4. Here we define an area as *old urban* if it is an urban area in the present and as *new urban* if it is not an urban area in the present but it is an urban area in the future scenario. Note that *urban shrinking* or the replacement of an urban cover to a non-urban surface was not assumed in this study.

When looking at the whole domain (in other words, at a large scale), the effect of urbanization can still be observed, however, it is relatively insignificant compared to the global effects. This is because in each domain, urban area covers only (13.2 $\pm$ 10.5) % of the whole domain size. Even when all water bodies are excluded, the ratio is still only (17.2 $\pm$ 11.8) %.

Focusing on the old urban, the effects of urbaniza-

Table 3 Root-mean-square error (RMSE, ℃), bias (℃), standard error (SE, ℃), and Pearson correlation coefficient (r) of simulated hourly 2 m air temperature. Note: $\text{RMSE}^2 = \text{Bias}^2 + \text{SE}^2$.

	RMSE	Bias	SE	r
Overall	2.01	0.98	1.76	0.96
Daytime	2.31	1.51	1.74	0.95
Nighttime	1.52	0.26	1.50	0.97
Individual cities	0.55 to 3.93	−2.11 to 3.58	0.54 to 2.56	0.81 to 0.99

Table 4 Mean and standard deviation of each domain's spatial mean of change in daily mean 2 m air temperature in intermediate scenario and future scenario with present scenario taken as the basis of comparison, and urbanization effect which is obtained by subtracting the change in intermediate scenario from the change in future scenario. Unit: ℃.

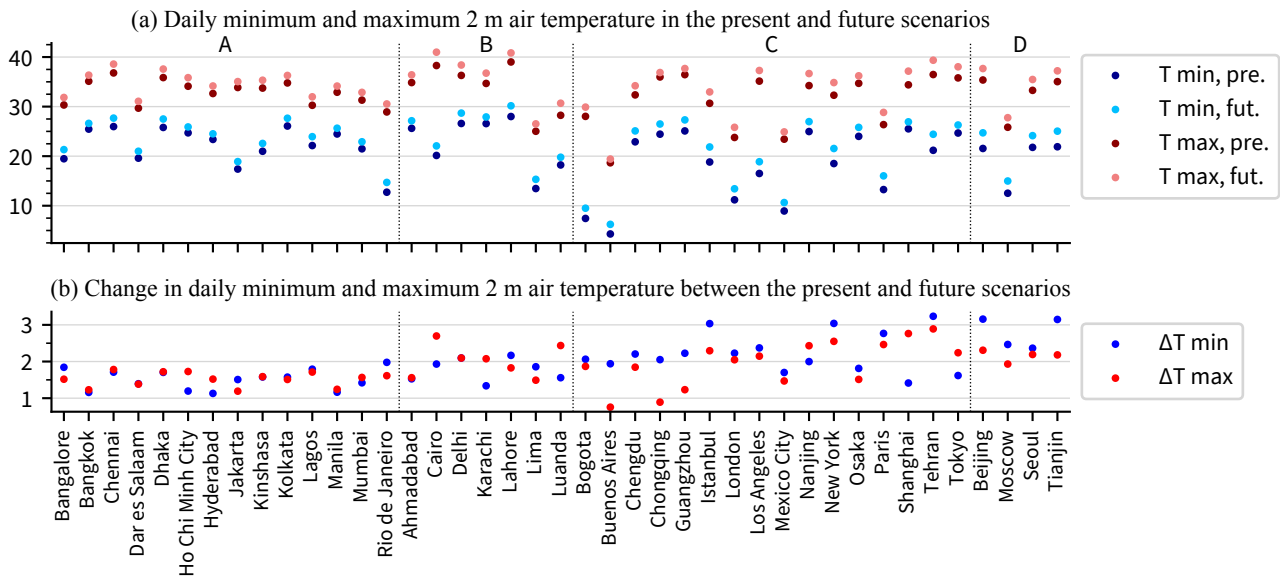| Focus	Scenario		Urbanization effect
	Intermediate	Future	
Domain	1.79 $\pm$ 0.47	1.84 $\pm$ 0.49	0.05 $\pm$ 0.05
Old urban	1.82 $\pm$ 0.51	1.91 $\pm$ 0.51	0.09 $\pm$ 0.11
New urban	1.85 $\pm$ 0.50	2.13 $\pm$ 0.54	0.28 $\pm$ 0.13

Fig. 2 Spatial daily minimum and maximum 2 m air temperature in urban areas in August in the present and future scenarios, and their difference. Domains are grouped by Köppen climate classification (A: tropical, B: dry, C: temperate, D: continental),[18] domains in the same group are sorted in lexicographical order. Unit: ℃.

tion becomes clearer with higher mean and also more variance than the whole domain. The large variance is due to the fact that the development in some old urban areas has been saturated (for example, Tokyo, Bangkok, and London) while it is still progressing rapidly in some others (for example, Dar es Salaam, Buenos Aires, and Kinshasa) as shown in Fig. 1.

The effect becomes clearest when looking at the new urban. The mean effect in the new urban is significantly higher than that in the whole domain and the old urban. The contribution of urbanization effect to the total temperature change in the new urban is (13.5 ± 5.9) %, which is not negligible. This clear effect is explainable by the fact that the formation of the new urban fundamentally changes the characteristics of land cover. Usually, the area of impermeable surface increases and vegetation fraction decreases. Consequently, there is less latent heat and more sensible heat, leading to the increase in air temperature.

Daily minimum and maximum temperature in urban areas in all domains in the present scenario, the future scenario and the difference between the two scenarios are summarized in Fig. 2. In 26 out of 41 domains, the increase in daily minimum temperature is higher than the increase in daily maximum temperature, implying a narrower diurnal temperature range (DTR) in the future. However, no correlation could be identified between present temperature statistics and change in DTR. In addition, the increase in daily maximum and minimum temperature is smallest in domains with tropical climate and highest in domains with continental climate. Further investigation is needed to understand mechanism of the difference between the increase of daily minimum temperature and that of daily maximum temperature, and the difference in the increase due to climate classification.

(3) Wind and urbanization effect on non-urban areas

By visually inspecting the two-dimensional distribution of urbanization effect and wind map, we found that in six domains (Luanda, Buenos Aires, Dar es Salaam, Karachi, Kinshasa, and Lagos), the effect of urbanization can be observed downwind. Specifically, going from the intermediate scenario to the future scenario, increase in air temperature was observed in non-urban areas (including water body) downwind of urban areas. This increase should be due to the hot air advected from the urban areas upwind.

For example, in Dar es Salaam (Fig. 3(a) and (b)), the phenomenon was observed clearly from evening to sunrise. The long red tail did not originate from the surface directly beneath it because the tail changed with wind direction and it lay on the ocean while both urbanization expansion and increase in anthropogenic heat do not happen on the ocean and they have no dependency on wind direction. As depicted in the figure, the urbanization effect could be advected by

Table 5 The time at which advected urbanization effect could be observed in local time.

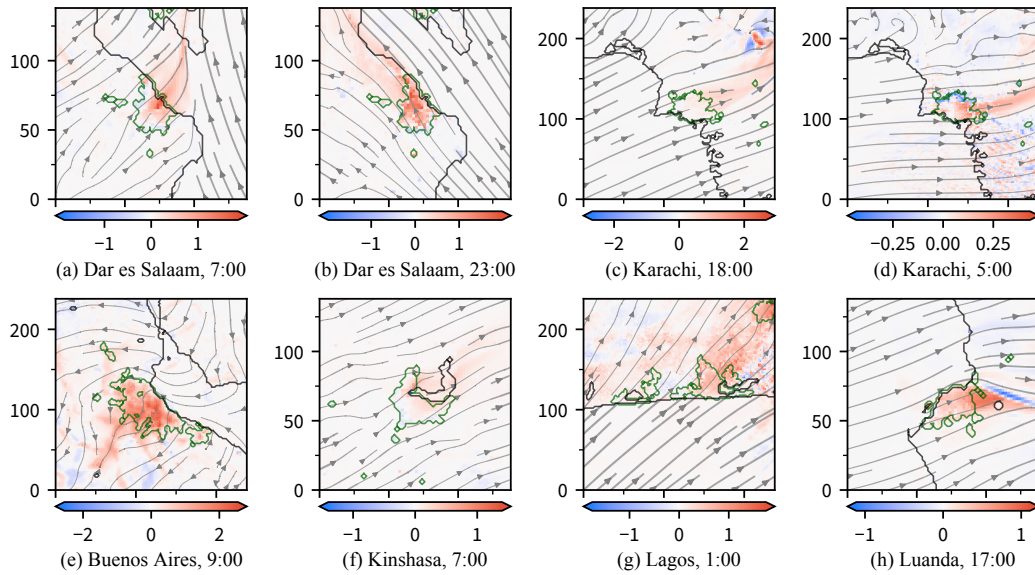| Domain	Time range	Domain	Time range
Buenos Aires	8:00 to 9:00	Kinshasa	7:00 to 8:00
Dar es Salaam	18:00 to 8:00	Lagos	22:00 to 5:00
Karachi	15:00 to 5:00	Luanda	17:00 to 21:00

Fig. 3 Urbanization effect advected by wind in different domains at different time averaged throughout the simulation period. Coastline and inland water body boundary are depicted by black line. Urban area boundary is depicted by green line. The effect is measured in °C, the unit of horizontal and vertical axes is km, the time is local time. In each figure, the scales of the axes are the same.
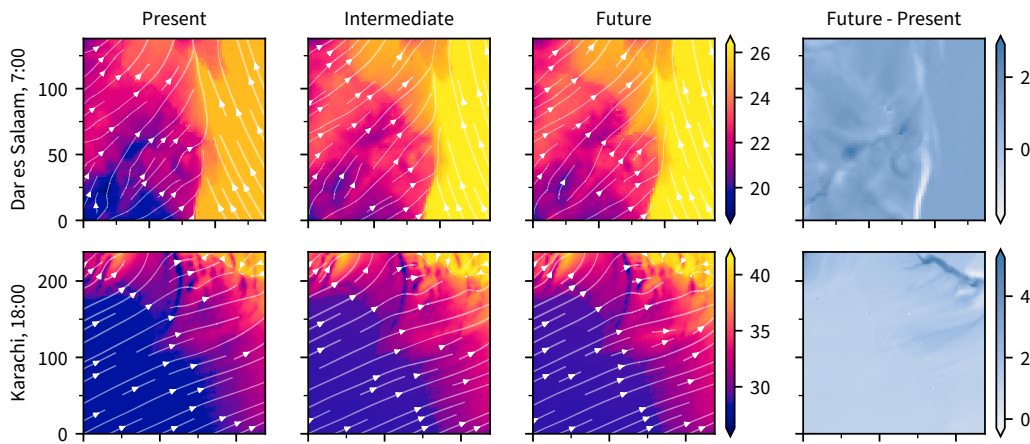

Fig. 4 2 m air temperature in Dar es Salaam at 7:00 and Karachi at 18:00 (local time) in the present, intermediate, and future scenario (averaged throughout the simulation period), and the difference between the present and the future scenario. The unit of temperature is °C, the unit of horizontal and vertical axes is km. In each figure, the scales of the axes are the same.

the wind up to 60 km downwind.

Fig. 4 shows the air temperature in Dar es Salaam and Karachi in the present, intermediate, and future scenario at the time the phenomenon could be observed clearly. However, looking at these temperature maps, no discernible difference could be seen. The phenomenon could not be identified even when looking at the map of temperature difference between the present and the future scenario due to its high uniformity. This justifies the necessity of simulating the intermediate scenario in evaluating the effect of urbanization.

The time at which the phenomenon could be observed is summarized in Table 5. The time varied but in general, the phenomenon could be observed from late afternoon to next day's early morning in August.

These domains share the same feature of having relatively simple wind patterns. Topography may play a role but neither wind pattern nor topography is the decisive cause because the phenomenon could be observed in Buenos Aires, which has relatively complex topography, but could not be observed in Ho Chi Minh City, which is a flat river delta, very close to sea level, and also has a simple wind pattern. This argument does not imply that the phenomenon does not exist in Ho Chi Minh City and 34 other domains but the phenomenon, if exists, could not be visually identified. Perhaps a systematic method to quantify this phenomenon is required. In addition, there are other factors that cannot be analyzed within the scope of this study such as seasonal dependency.

4. CONCLUSION

In this study, we projected 2 m air temperature change for 43 megacities in August between the 2006–2015 period (present period) and the 2046–2055 period (future period) using PGW method under the assumptions of uncontrolled urban expansion, RCP8.5 emission forcing, and SSP3 which we interpreted as the worst case scenario for the future.

Quantification of urbanization effect indicated that the effect is observable but negligible at large spatial scale, clearer in old urban area with large variance between saturated old urban and rapidly developing old urban. The effect is clearest and significant in new urban area. We also found that under certain conditions, urbanization effect in urban area can be advected by the wind resulting urbanization effect in faraway non-urban areas.

A limitation of this study is that instead of conducting simulations for the full month of August in ten years, we conducted simulations using ensemble averaged August days repeatedly. One direction for future study is to compare the results of these two approaches.

This study can be further extended by considering other months, other emission forcing, and other socioeconomic pathways. However, these extensions require adjustment of the urban sprawling map and anthropogenic heat emission map accordingly. Study focusing on individual cities will remain very important to adapt to specific needs that the method used in this study cannot cover. They will also serve as reinforcement for further development of this global approach.

REFERENCES

1) United Nations. (2018). *The world's cities in 2018: Data booklet*. doi:10.18356/c93f4dc6-en
2) Adachi, S. A., Kimura, F., Kusaka, H., Inoue, T., & Ueda, H. (2012). Comparison of the impact of global climate changes and urbanization on summertime future climate in the Tokyo metropolitan area. *J. Appl. Meteorol. Climatol. 51*(8), 1441–1454. doi:10.1175/JAMC-D-11-0137.1
3) Argüeso, D., Evans, J. P., Fita, L., & Bormann, K. J. (2014). Temperature response to future urbanization and climate change. *Clim. Dyn. 42*, 2183–2199. doi:10.1007/s00382-013-1789-6
4) Doan, Q.-V., Kusaka, H., & Ho, Q.-B. (2016). Impact of future urbanization on temperature and thermal comfort index in a developing tropical city: Ho Chi Minh City. *Urban Clim. 17*, 20–31. doi:10.1016/j.uclim.2016.04.003
5) Darmanto, N. S., Varquez, A. C. G., Kawano, N., & Kanda, M. (2019). Future urban climate projection in a tropical megacity based on global climate change and local urbanization scenarios. *Urban Clim. 29*, 100482. doi:10.1016/j.uclim.2019.100482
6) Kimura, F., & Kitoh, A. (2007). Downscaling by pseudo global warming method. *The Final Report of ICCAP*, *4346*.
7) Narita, Y., Varquez, A. C. G., Nakayoshi, M., & Kanda, M. (2019). Construction of land use database before urbanization for global urban climate analysis. *J. Jpn. Soc. Civ. Eng., Ser. B1 (Hydraul. Eng.) 75*(2), I_1039–I_1044.
8) Varquez, A. C. G., Darmanto, N., Kawano, N., Takakuwa, S., Kanda, M., & Xin, Z. (2017). Representative urban growing scenarios for future climate models. *J. Jpn. Soc. Civ. Eng., Ser. B1 (Hydraul. Eng.) 73*(4), I_103–I_108. doi:10.2208/jscejhe.73.i_103
9) Varquez, A. C. G., Nakayoshi, M., & Kanda, M. (2015). The effects of highly detailed urban roughness parameters on a sea-breeze numerical simulation. *Bound.-Layer Meteorol. 154*, 449–469. doi:10.1007/s10546-014-9985-4
10) Dong, Y., Varquez, A. C. G., & Kanda, M. (2017). Global anthropogenic heat flux database with high spatial resolution. *Atmos. Environ. 150*, 276–294. doi:10.1016/j.atmosenv.2016.11.040
11) Kiyomoto, S., Varquez, A. C. G., & Kanda, M. (2018). Anthropogenic heat flux distribution with point sources for global urban climatology. *J. Jpn. Soc. Civ. Eng., Ser. B1 (Hydraul. Eng.) 74*(5), I_1171–I_1176. doi:10.2208/jscejhe.74.5_I_1171
12) Varquez, A. C. G., Takakuwa, S., Kanda, M., & Xin, Z. (2018). Future population distribution of an urban agglomeration given climate change scenarios. *J. Jpn. Soc. Civ. Eng., Ser. B1 (Hydraul. Eng.) 74*(4), I_223–I_228. doi:10.2208/jscejhe.74.I_223
13) Zhou, Y., Varquez, A. C. G., & Kanda, M. (2019). High-resolution global urban growth projection based on multiple applications of the SLEUTH urban growth model. *Sci. Data, 6*, 34. doi:10.1038/s41597-019-0048-z
14) Riahi, K., van Vuuren, D. P., Kriegler, E., Edmonds, J., O'Neill, B. C., Fujimori, S., … Tavoni, M. (2017). The shared socioeconomic pathways and their energy, land use, and greenhouse gas emissions implications: An overview. *Glob. Environ. Change, 42*, 153–168. doi:10.1016/j.gloenvcha.2016.05.009
15) KC, S., & Lutz, W. (2017). The human core of the shared socioeconomic pathways: Population scenarios by age, sex and level of education for all countries to 2100. *Glob. Environ. Change, 42*, 181–192. doi:10.1016/j.gloenvcha.2014.06.004
16) Dellink, R., Chateau, J., Lanzi, E., & Magné, B. (2017). Long-term economic growth projections in the shared socioeconomic pathways. *Glob. Environ. Change, 42*, 200–214. doi:10.1016/j.gloenvcha.2015.06.004
17) Cuaresma, J. C. (2017). Income projections for climate change research: A framework based on human capital dynamics. *Glob. Environ. Change, 42*, 226–236. doi:10.1016/j.gloenvcha.2015.02.012
18) Rubel, F., & Kottek, M. (2010). Observed and projected climate shifts 1901–2100 depicted by world maps of the Köppen-Geiger climate classification. *Meteorol. Z. 19*(2), 135–141. doi:10.1127/0941-2948/2010/0430